LETTERS

# Rapid sea-level rise and reef back-stepping at the close of the last interglacial highstand

Paul Blanchon[1], Anton Eisenhauer[2], Jan Fietzke[2] & Volker Liebetrau[2]

**Widespread evidence of a +4–6-m sea-level highstand during the last interglacial period (Marine Isotope Stage 5e) has led to warnings that modern ice sheets will deteriorate owing to global warming and initiate a rise of similar magnitude by AD 2100 (ref. 1). The rate of this projected rise is based on ice-sheet melting simulations and downplays discoveries of more rapid ice loss[2,3]. Knowing the rate at which sea level reached its highstand during the last interglacial period is fundamental in assessing if such rapid ice-loss processes could lead to future catastrophic sea-level rise. The best direct record of sea level during this highstand comes from well-dated fossil reefs in stable areas[4–6]. However, this record lacks both reef-crest development up to the full highstand elevation, as inferred[7] from widespread intertidal indicators at +6 m, and a detailed chronology, owing to the difficulty of replicating U-series ages on submillennial timescales[8]. Here we present a complete reef-crest sequence for the last interglacial highstand and its U-series chronology from the stable northeast Yucatán peninsula, Mexico. We find that reef development during the highstand was punctuated by reef-crest demise at +3 m and back-stepping to +6 m. The abrupt demise of the lower-reef crest, but continuous accretion between the lower-lagoonal unit and the upper-reef crest, allows us to infer that this back-stepping occurred on an ecological timescale and was triggered by a 2–3-m jump in sea level. Using strictly reliable $^{230}$Th ages of corals from the upper-reef crest, and improved stratigraphic screening of coral ages from other stable sites, we constrain this jump to have occurred ~121 kyr ago and conclude that it supports an episode of ice-sheet instability during the terminal phase of the last interglacial period.**

Reconstruction of eustatic sea level from the precise age and elevation of submerged reef-crest corals has shown that the last deglaciation (Termination 1) was punctuated by rapid, metre-scale rise events caused by ice-sheet instability[9–12]. Little is known, however, about the potential for unstable ice-sheet and sea-level behaviour within fully interglacial climates. The Holocene interglacial has been relatively stable, but the picture of sea-level variation during the last interglacial is less clear, owing to greater chronological uncertainty[8]. There is circumstantial evidence that it was punctuated by instability both during the preceding deglaciation[13] and, more unexpectedly, during the highstand[7]. For example, highstand reef sequences in uplifted terraces show double-reef architectures, marine erosion surfaces and coral age–depth relationships suggestive of significant relative sea-level excursions[14–16]. However, coseismic displacement and intraterrace faulting cannot be discounted as a cause of relative sea-level variability in such active terranes. Sea-level instability has also been inferred from an isotopic reconstruction from the Red Sea[17], but these data have large uncertainties and are inconsistent with coral-based sea-level data from stable areas (Supplementary Discussion).

In these stable areas, well-dated reef terraces are developed to +3 m (refs 4–6), but intertidal deposits and notches indicate that sea level reached +5–6 m during the highstand[7]. This absence of reefs above +3 m, along with the presence of similar erosion surfaces, has also been interpreted as evidence of sea-level excursions both during and terminating the highstand[7,18]. Without a complete reefal sequence to +6 m, however, a convincing case for sea-level instability cannot be made. Pervasive open-system diagenesis makes it unlikely that the duration or rate of submillennial sea-level events can be radiometrically constrained during the last interglacial, as they are for Termination 1, but rapid accretion combined with a predictable depth zonation of coral and encruster assemblages[19] means that reefs respond to and preserve extrinsic changes on ecological (decadal) timescales[20], making them ideal for identifying rapid changes in eustatic sea level associated with ice-sheet instability[10].

To investigate possible submillennial changes in sea level during the last interglacial highstand, we analysed the stratigraphic architecture, palaeoecologic zonation and $^{230}$Th age structure of an exceptionally well-exposed fossil reef at Xcaret, a theme park on the northeast coast of the Yucatán peninsula. The northern part of the peninsula is an ideal location at which to investigate sea-level behaviour because it is historically aseismic[21] and lacks neotectonic activity[22], as confirmed by both its thick, surficial off-lapping sequence of undeformed Miocene to Pleistocene carbonates and its +6-m last interglacial shoreline[23]. In addition, the conformity of this highstand elevation with other stable sites across the Caribbean[7] indicates that the glacio-isostatic state of the peninsula, relative to an equilibrium state, was similar to the present[24] and that submillennial changes in relative sea-level history should accurately reflect a eustatic signature.

We measured 40 vertical sections and examined ~2.5 km of lateral exposure through the fossil reef (Fig. 1). For the first time in a stable area, these sections show a complete reefal sequence, consisting of two separate linear reef tracts with reef crests that are offset and at different elevations (Supplementary Fig. 1). The lower-reef tract crops out along northern shore for ~500 m and its reef crest extends from below mean sea level to +3 m. Like modern reefs[19], the crest consists of large *A. palmata* colonies dispersed within an *A. palmata* boulder gravel; this is flanked by a reef front with a mixed coral assemblage and a large, lagoonal patch-reef complex. The upper-reef tract crops out ~150 m inland and parallels the southern section of shore for ~400 m. The reef crest, which also consists of large *A. palmata* colonies and its boulder-sized clasts, is developed between +3 and +5.8 m and is founded directly upon the lagoonal patch-reef complex of the lower tract. Both reef tracts are overlain by a regressive beach unit that prograded down slope as sea level fell from the highstand.

To distinguish chronologically between these two stages of reef-tract development, we obtained $^{230}$Th ages in triplicate from ten well-preserved coral samples, five from each tract (Supplementary Table 1). From the lower reef, two subsamples (xA4-2b and xA4-2c) gave isotopically reliable ages (Methods). By contrast, all five samples

[1]Institute of Marine & Limnological Sciences, National Autonomous University of Mexico, AP1152, Cancun, 77500 Quintana Roo, Mexico. [2]Leibniz Institute of Marine Science, IFM-GEOMAR, Wischhofstrasse 1–3, 24148 Kiel, Germany.

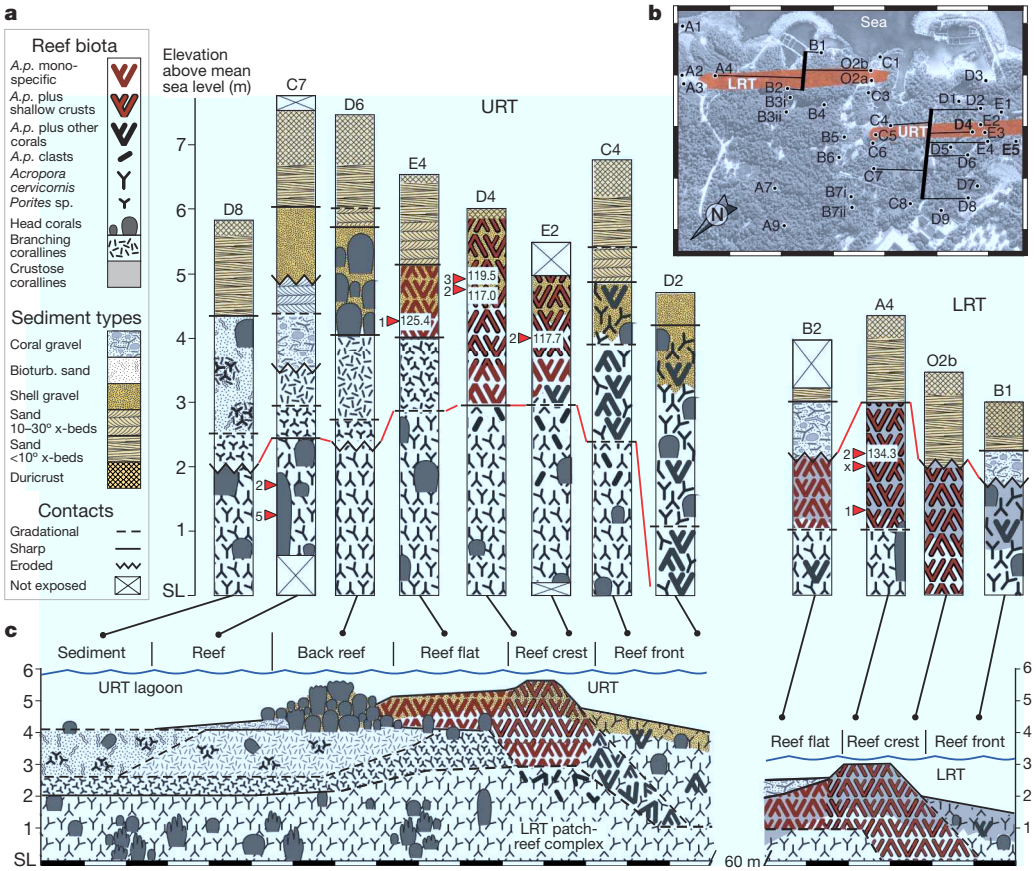


**Figure 1 | Stratigraphic sections and reconstruction of reef development at Xcaret during the last interglacial.** **a**, Stratigraphic sections along transects crossing *Acropora palmata* (*A.p.*) reef crests, showing age, geometry, elevation and contact relations of the upper-reef tract (URT) and the lower-reef tract (LRT) (red line marks boundary). Positions of dated coral samples (ages in kiloyears) are indicated by red arrowheads (only strictly reliable ages shown). x-bed, cross-bedding. **b**, Location of transects, stratigraphic sections (all detailed in Supplementary Fig. 1) and subcrop positions of reef-crest units from the LRT and the URT. Scale, 100 m. **c**, Reconstruction of zonation, geometry and elevation of the LRT and the URT and their corresponding sea-level positions (overlying regressive beach unit omitted for clarity). Horizontal scale, 10 m.

from the upper reef gave at least one age that is isotopically reliable (Fig. 2). These reliable $^{230}$Th ages confirm that both reef tracts are contemporary and formed during Marine Isotope Stage 5e. However, the reliable subsamples from upper-reef corals reveal a millennial-scale age variability that exceeds the analytical error by a factor of 3–10—a finding that is consistent with other analyses of true-age variability[8]. To address this variability, we excluded subsamples with $\delta^{234}U(T)$ values outside the range of modern corals and sea water (146.6–149.6‰)[25]. This left two strictly reliable ages from the lower reef and five strictly reliable ages from the upper reef (Fig. 2 and Supplementary Table 1). The two ages from the lower reef, 132 and 134 kyr, indicate that it is older than the upper reef, but, given the marginal $^{238}$U concentrations, their accuracy is suspect. Ages from the upper reef show a range between 125 and 117 kyr, but the older ages are from clasts of *A. palmata* in the reef-flat zone, and could potentially be transported from the lower reef by hurricanes (thus making them unreliable for sea-level determination). The two strictly reliable subsamples from *in situ A. palmata* colonies in the reef crest (xD4-2a and xD4-3a) gave younger ages, between 117 and 119.5 kyr, and most likely indicate the true age of upper-reef tract development (Fig. 2). The only other *in situ* coral dated from the upper-reef crest (xE2-2a) also gave an age of 117.7 kyr, but this is accurate only to within 2 kyr.

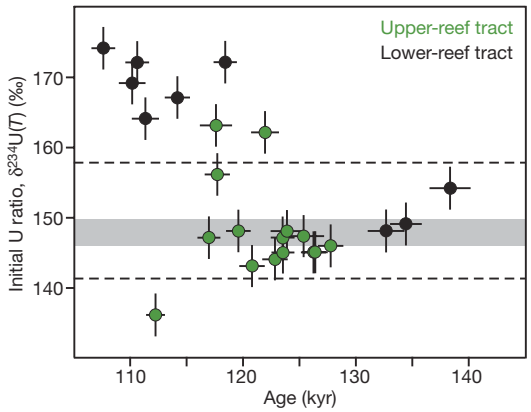


**Figure 2 | Isotopic reliability of $^{230}$Th coral ages from Xcaret.** Ages within the grey band (146.6–149.6‰) have the same $\delta^{234}U(T)$ value as modern corals and sea water and are strictly reliable. $\delta^{234}U(T)$ represents the decay-corrected activity ratio calculated from the value measured today ($T = 0$): $\delta^{234}U(T) = \delta^{234}U(0)\exp(\lambda_{234}T)$, where $\delta^{234}U(0)$ (‰) $= [(^{234}U/^{238}U)_{activity} - 1] \times 10^3$ and $\lambda_{234} = 2.8263 \times 10^{-6}$ yr$^{-1}$. Ages within the dashed lines correspond to 149 ± 8‰ and are isotopically reliable to within 2 kyr (Methods). All other ages are unreliable. Error bars, two standard deviations of the mean ($2\sigma$).

Despite the lack of a good age from the lower-reef tract, differences in biofacies and elevation confirm that the two reefs are contemporaneous and had a back-stepping pattern of development. Progradation of the overlying beach unit during sea-level fall at the end of the highstand, for example, caused infiltration of an abraded shell gravel into the upper-reef crest and adjacent zones. This indicates that the reef had an open framework and was alive just before sea-level fell. No infiltration of beach gravel occurred in the lower-reef crest, however, because surface porosity was already occluded by a cap of crustose coralline algae (Fig. 1). This lack of infiltration requires that the lower reef be older, and the presence of a coralline cap signifies that

it died suddenly but remained submerged in sea water. Combined with its greater elevation, these differences imply that the upper reef back-stepped during sea-level rise.

The timing of reef demise and back-stepping is further constrained by key differences in the stratigraphic transition between the two reef tracts. In the lagoon, the transition is discontinuous and marked by a sharp, erosive contact across which there is a switch from patch-reef corals to sediment-tolerant intergrowths of branching coralline algae[26] and small-branched *Porites* (see D8 to D6, Fig. 1). By contrast, on the adjacent but more elevated windward edge of the patch-reef complex, the transition into the upper crest is abrupt but continuous, implying that conditions changed rapidly but remained conducive to continuous coral growth (see E4 to C4, Fig. 1). The sudden demise of reef-crest corals in the lower reef was therefore not only accompanied by sudden, partial demise in the lagoon, but also by a sudden ecological shift to reef-crest conditions along the windward edge of the patch-reef complex. This continuous development between reef tracts not only requires that they were contemporaneous but that the demise of the lower-reef crest at +3 m was ecologically synchronous with back-stepping and relocation of the upper-reef crest (Fig. 1c).

Furthermore, sea-level indicators demonstrate that this abrupt reef-crest back-stepping occurred at a sea-level position that was higher by 2–3 m. We assume that the maximum elevation of the lower-reef crest at +3 m closely represents mean low water and rule out the possibility that it was a submerged feature on the basis of the distinct breakwater facies zonation and the development of a lagoon where patch reefs reached the same elevation (Fig. 1c and Supplementary Fig. 1). The conclusion that this was a breakwater reef is also supported by the presence of a shallow, depth-restricted encruster association[19] of coralline algae, *Homotrema rubrum* and vermetid gastropods on clasts and colonies of *A. palmata*.

The upper-reef crest, by contrast, contains clear indicators of a sea-level position higher than +3 m during its earliest development. *In situ* colonies of *A. palmata* up to 1.5 m tall are developed at the base of the reef-crest unit between +3 and +4.5 m (see D4 and E2, Fig. 1). If those colonies reached mean low water, then sea level must have been a minimum of +4.5 m when the crest developed. This higher sea-level position is also supported by the +4–4.5-m elevation of the base of the reef-flat deposit, which indicates that it could only have developed at a sea-level position greater than or equal to +4.5 m (see E4, D5 and C5, Supplementary Fig. 1). Finally, the reef-crest encruster association only appears above an elevation of +3.5 m, which is consistent with a sea-level position of +5.5 m. Combined, these indicators provide reliable evidence for a minimum sea-level position of +5 m during early development of the upper-reef tract. We note, however, that the upper reef-flat surface at +5.5 m is close to the maximum reef-crest elevation of +5.8 m. The possibility that sea level jumped from +3 m to its final highstand elevation of +6 m cannot therefore be excluded (Fig. 1).

Given the absence of widespread reef development above +3 m in stable, low-lying areas like the Bahamas and Western Australia, the complete reef section at Xcaret provides a key insight into the final stage of reef development during the last interglacial. Reef demise and back-stepping at Xcaret was not only accompanied by localized erosion in the lagoon, but also by an abrupt switch to a sediment-tolerant assemblage[26]. This implies that the 2–3-m sea-level jump outpaced accretion of the lower-reef crest and created a higher-energy wave field that enhanced sediment flux and smothered and eroded corals in lagoonal depressions. Coral growth could only continue along the elevated edge of the patch-reef complex and quickly developed large colonies of *A. palmata*, which formed the core of the upper-reef crest. This single jump in sea-level was therefore responsible for reef demise, marine erosion, back stepping and the suppression of reef growth—features that are all common along other low-lying coasts and that have been used to support claims of multiple sea-level excursions during the last interglacial[7] (Supplementary Discussion).

To constrain the timing of the sea-level jump during the last interglacial, we screened isotopically reliable ages from the Bahamas[4] and Western Australia[5,6] for stratigraphic consistency[27] (Methods) and compared these data with coral ages and reef-crest sea-level indicators from Xcaret (Fig. 3). We identified three stratigraphically reliable age groups from the extensive Western Australia data set which indicate that widespread reef development at +3 m occurred during a 5-kyr stillstand of sea level between 126 and 121 kyr ago (Fig. 3). Most of the reliable ages of corals from the Bahamas fall into the same interval but do not form stratigraphically consistent groups. Given the limited occurrence of reef development up to +6 m in these stable areas, and the younger age of *in situ* reef-crest corals from the upper reef at Xcaret, we tentatively place the timing of the sea-level jump that caused reef demise and back-stepping at Xcaret immediately after the youngest reliable age group, 121 kyr ago. Although the precision of these ages precludes any direct measurement of the rise rate involved in the jump, it was most likely similar to rates that caused ecologically sudden demise and back-stepping of Caribbean reefs during the last

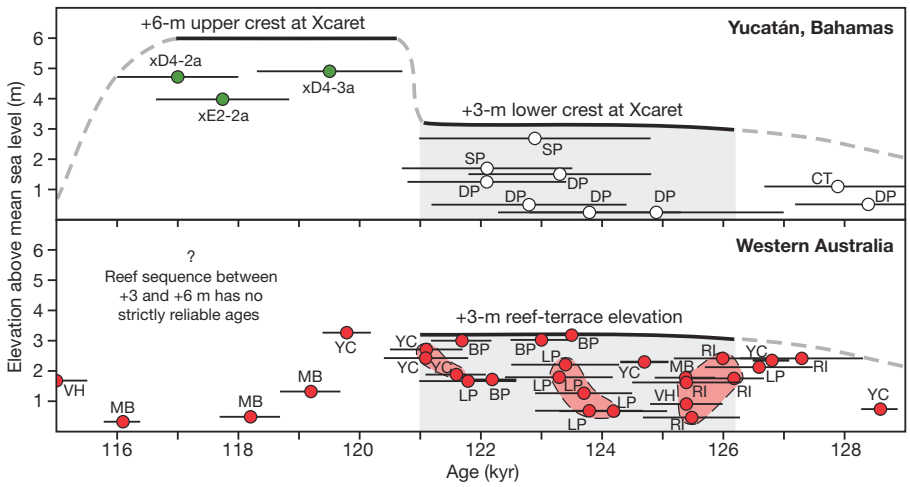


**Figure 3 | Relative sea-level reconstructions for the last interglacial highstand.** Open circles are isotopically reliable ages from the Bahamas[4]. (CT, Cockburn Town, San Salvador; SP, Sue Point, San Salvador; DP, Devil's Point, Great Inagua). Green circles are isotopically reliable ages from *in situ* upper-reef-crest corals at Xcaret. Sea-level position is defined by surface elevation of Xcaret reef-crest units. Red circles are isotopically reliable ages from Western Australia[5,6]. (VH, Vlaming Head; MB, Mangrove Bay; YC, Yardie Creek; BP, Burney Point; LP, Leander Point; RI, Rottnest Island.) Sea-level position is defined by surface elevation of the reef terrace. Stratigraphically consistent age groups highlighted in Western Australia data define a 5-kyr interval for the +3-m sea-level stillstand (shaded interval). Error bars, 2$\sigma$.

deglaciation[10,12]. During those jumps, direct measurement of rise rates shows that they exceeded 36 mm $yr^{-1}$ (refs 10, 28; see Supplementary Fig. 3). Our discovery of an ecologically sudden demise and back-stepping signature in reef-crest deposits from the Yucatán is therefore compelling evidence for a sea-level jump with a similar rise rate during the late stages of the last interglacial. This jump implies that an episode of ice-sheet instability, characterized by rapid ice loss, occurred late during an interglaciation that was warmer than present.

In our warming world, the implications of a rapid, metre-scale sea-level jump late during the last interglacial are clear for both future ice-sheet stability and reef development. Given the dramatic disintegration of ice shelves[2] and discovery of rapid ice loss from both the Antarctic and Greenland ice sheets[3], the potential for sustained rapid ice loss and catastrophic sea-level rise in the near future is confirmed by our discovery of sea-level instability at the close of the last interglacial. Furthermore, the inhibition of reef development that this instability caused has negative implications for the future viability of modern reefs, which are already being impacted by anthropogenic activity on a global scale[29].

## METHODS SUMMARY

We characterized detrital, framework and encruster facies in reef stratigraphic sections following ref. 19, and recorded contact types and elevations using a sea-level datum (±15 cm). Lateral continuity of units was physically traced between sections.

U-series measurements on coral samples used multistatic, multi-ion-counting inductively coupled plasma mass spectroscopy, following ref. 30. Whole-procedure blank values of the measured sample set were ~2 pg for Th and 4–8 pg for U, both typical of this method and laboratory.

We based isotopic screening for potential U and Th loss or gain on several standard criteria[8]: the $^{238}U$ concentration should reflect modern coral species values (2.0–3.5 p.p.m.), the $^{232}Th$ concentration should be <2 p.p.b. and the abundance of calcite must be below X-ray diffraction detection limits. For samples meeting these criteria, age reliability is based on the $\delta^{234}U(T)$ criterion. We considered ages with the same $\delta^{234}U(T)$ value as modern corals and sea water (146.6–149.6‰)[25] to be strictly reliable to within the analytical uncertainty; ages with values of 149 ± 8‰ were considered to be accurate to ±2 kyr (refs 4, 6, 13, 14), and ages with values >149 ± 8‰ were considered to be unreliable.

Combined $^{230}Th$ and $^{231}Pa$ dating has shown that the $\delta^{234}U(T)$ criterion alone is insufficient to identify all corals affected by open-system diagenesis[8]. Quantification of extrinsic age variability in Holocene reefs has recently provided a criterion for screening isotopically reliable ages for stratigraphic consistency[27]. This is based on the finding that a minimum of three corals growing within a 3-m vertical stratigraphic interval should not have an age distribution of >1 kyr. As a result, we consider the ages of groups of three or more corals that vary by no more than 1 kyr and come from conformable stratigraphic sections no thicker than 3 m to be stratigraphically reliable.

**Full Methods** and any associated references are available in the online version of the paper at www.nature.com/nature.

**Received 8 October 2008; accepted 23 February 2009.**


1. Overpeck, J. T. *et al.* Paleoclimatic evidence for future ice-sheet instability and rapid sea-level rise. *Science* **311,** 1747–1750 (2006).
2. Thomas, R. *et al.* Accelerated sea-level rise from West Antarctica. *Science* **306,** 255–258 (2004).
3. Bamber, J. L., Alley, R. B. & Joughin, I. Rapid response of modern day ice sheets to external forcing. *Earth Planet. Sci. Lett.* **257,** 1–13 (2007).
4. Chen, J. H., Curran, H. A., White, B. & Wasserburg, G. J. Precise chronology of the last interglacial period: $^{234}U$-$^{230}Th$ data from fossil coral reefs in the Bahamas. *Geol. Soc. Am. Bull.* **103,** 82–97 (1991).
5. Stirling, C., Esat, T., McCulloch, M. & Lambeck, K. High-precision U-series dating of corals from Western Australia and implications for the timing and duration of the last interglacial. *Earth Planet. Sci. Lett.* **135,** 115–130 (1995).
6. Stirling, C., Esat, T., Lambeck, K. & McCulloch, M. Timing and duration of the last interglacial: evidence for a restricted interval of widespread coral reef growth. *Earth Planet. Sci. Lett.* **160,** 745–762 (1998).
7. Neumann, A. C. & Hearty, P. J. Rapid sea-level changes at the close of the last interglacial (substage 5e) recorded in Bahamian island geology. *Geology* **24,** 775–778 (1996).
8. Scholz, D. & Mangini, A. How precise are U-series coral ages? *Geochim. Cosmochim. Acta* **71,** 1935–1948 (2007).
9. Fairbanks, R. G. A 17,000-year long glacio-eustatic sea level record: influence of glacial melting rates on the Younger Dryas event and deep-ocean circulation. *Nature* **342,** 637–642 (1989).
10. Blanchon, P. & Shaw, J. Reef drowning during the last deglaciation: evidence for catastrophic sea-level rise and ice-sheet collapse. *Geology* **23,** 4–8 (1995).
11. Bard, E. *et al.* Deglacial sea-level record from Tahiti corals and the timing of global meltwater discharge. *Nature* **382,** 241–244 (1996).
12. Blanchon, P., Jones, B. & Ford, D. C. Discovery of a submerged relic reef and shoreline off Grand Cayman: further support for an early Holocene jump in sea level. *Sedim. Geol.* **147,** 253–270 (2002).
13. Esat, T., McCulloch, M., Chappell, J., Pillans, B. & Omura, A. Rapid fluctuations in sea level recorded at Huon Peninsula during the penultimate deglaciation. *Science* **283,** 197–201 (1999).
14. Stein, M. *et al.* TIMS U-series dating and stable isotopes of the last interglacial event in Papua New Guinea. *Geochim. Cosmochim. Acta* **57,** 2541–2554 (1993).
15. Bruggemann, J. H. *et al.* Stratigraphy, palaeoenvironments and model for the deposition of the Abdur Reef Limestone: context for an important archaeological site from the last interglacial on the Red Sea coast of Eritrea. *Palaeogeogr. Palaeoclimatol. Palaeoecol.* **203,** 179–206 (2004).
16. Thompson, W. G. & Goldstein, S. L. Open-system coral ages reveal persistent suborbital sea-level cycles. *Science* **308,** 401–404 (2005).
17. Rohling, E. J. *et al.* High rates of sea-level rise during the last interglacial period. *Nature Geosci.* **1,** 38–42 (2008).
18. Wilson, M., Curran, H. & White, B. Paleontological evidence of a brief global sea-level event during the last interglacial. *Lethaia* **31,** 241–250 (1998).
19. Blanchon, P. & Perry, C. T. Taphonomic differentiation of *Acropora palmata* facies in cores from Campeche Bank Reefs, Gulf of Mexico. *Sedimentology* **51,** 53–76 (2004).
20. Aronson, R. B., Macintyre, I. G. & Precht, W. F. Event preservation in lagoonal reef systems. *Geology* **33,** 717–720 (2005).
21. Zúñiga, F. R., Reyes, M. A. & Valdés, C. A general overview of the catalog of recent seismicity compiled by the Mexican Seismological Survey. *Geofís. Int.* **39,** 161–170 (2000).
22. Marquez-Azua, B., Cabral-Cano, E., Correa-Mora, F. & DeMets, C. A model for Mexican neotectonics based on nationwide GPS measurements, 1993–2001. *Geofís. Int.* **43,** 319–330 (2004).
23. Szabo, B. J., Ward, W. C., Weidie, A. E. & Brady, M. J. Age and magnitude of the late Pleistocene sea-level rise on the eastern Yucatan Peninsula. *Geology* **6,** 398–406 (1978).
24. Potter, E.-K. & Lambeck, K. Reconciliation of sea-level observations in the Western North Atlantic during the last glacial cycle. *Earth Planet. Sci. Lett.* **217,** 171–181 (2003).
25. Delanghe, D., Bard, E. & Hamelin, B. New TIMS constraints on the uranium-238 and uranium-234 in seawaters from the main ocean basins and the Mediterranean Sea. *Mar. Chem.* **80,** 79–93 (2002).
26. Steneck, R., Macintyre, I. & Reid, R. A unique algal ridge system in the Exuma Cays, Bahamas. *Coral Reefs* **16,** 29–37 (1997).
27. Edinger, E. N., Burr, G. S., Pandolfi, J. M. & Ortiz, J. C. Age accuracy and resolution of Quaternary corals used as proxies for sea level. *Earth Planet. Sci. Lett.* **253,** 37–49 (2007).
28. Peltier, W. R. & Fairbanks, R. G. Global glacial ice volume and Last Glacial Maximum duration from an extended Barbados sea level record. *Quat. Sci. Rev.* **25,** 3322–3337 (2006).
29. Hoegh-Guldberg, O. *et al.* Coral reefs under rapid climate change and ocean acidification. *Science* **318,** 1737–1742 (2007).
30. Fietzke, J., Liebetrau, V., Eisenhauer, A. & Dullo, C. Determination of uranium isotope ratios by multi-static MIC-ICP-MS: method and implementation for precise U- and Th-series isotope measurements. *J. Anal. At. Spectrom.* **20,** 395–401 (2005).


**Supplementary Information** is linked to the online version of the paper at www.nature.com/nature.

**Acknowledgements** We thank M. Sanchez, E. Rios and R. Raigoza for providing park access and hospitality; E. Jordan-Dahlgren for original descriptions of the aquarium trench; G. Jordan-Garza and I. Pino for field assistance; A. Kolevica and K. Fischer von Mollard for help with the $^{230}Th$ measurements; and C. Neumann, P. Hearty, C. Holmden, D. Hopley, A. Curran and W. C. Ward for discussions. Funding was provided by DGAPA grant IN218799.

**Author Contributions** P.B. initiated the study, collected and analysed the field data and wrote the manuscript. A.E., J.F. and V.L. performed the U-series and X-ray diffraction analyses, and A.E. discussed the results and commented on the manuscript.

**Author Information** Reprints and permissions information is available at www.nature.com/reprints. Correspondence and requests for materials should be addressed to P.B. (blanchon@icmyl.unam.mx).

## METHODS

**Stratigraphy.** Reef stratigraphic sections were measured using a sea-level datum and thus have a potential elevation error of ±15 cm corresponding to the spring tide amplitude. (That is, all sections intersected the water table, which has a hydraulic gradient of 7–10 mm $km^{-1}$ (ref. 31). In coastal areas such as Xcaret, it is equivalent to mean sea level and oscillates with the tidal cycle with no apparent lag[31].) Sections were logged by differentiating detrital carbonate facies from framework facies and recording their contact types and elevations. We performed characterization of detrital and framework facies following ref. 19. The lateral continuity of these units was physically traced between sections using an extensive network of Park tunnels and excavations. Full data on the sedimentology and stratigraphy will be published in a companion paper.

**Chronology.** U-series measurements of coral ages were performed at the Leibniz Institute of Marine Sciences at the University of Kiel (IFM-GEOMAR). Element separation procedure follows previously published methods but used Eichrom-UTEVA resin[30]. Determination of U and Th isotope ratios followed a multistatic, multi-ion-counting inductively coupled plasma mass spectroscopy approach[30]. For isotope dilution measurements, a combined $^{233}U/^{236}U/^{229}Th$ spike was used, with stock solutions calibrated for concentration using NIST-SRM 3164 (U) and NIST-SRM 3159 (Th) and, as combi-spike, calibrated against CRM-145 uranium standard solution (also known as NBL-112A) for U isotope composition and against a secular equilibrium standard (HU-1, uranium ore solution) for the precise determination of $^{230}Th/^{234}U$ activity ratios. Whole-procedure blank values of this sample set were measured to be around 2 pg for Th and between 4 and 8 pg for U. Both values are in the range typical of this method and the laboratory.

Isotopic screening for potential U and Th loss or gain was based on several standard criteria[8]: the calculated $\delta^{234}U(T)$ values should lie within the range of modern corals and sea-water, between 146.6 ± 1.4‰ and 149.6 ± 1.0‰ (ref. 25); the $^{238}U$ concentration should reflect modern coral species values of between 2.0 and 3.5 p.p.m.; the $^{232}Th$ concentration should be <2 p.p.b.; and the abundance of calcite must be below X-ray diffraction detection limits (<1% calcite). For samples within the $^{238}U$ and $^{232}Th$ concentration ranges, and which lack detectable calcite, the reliability of coral ages is based on the $\delta^{234}U(T)$ criterion: ages with the same $\delta^{234}U(T)$ value as pristine modern coral and sea water (146.6–149.6‰) are considered to be strictly reliable to within the analytical uncertainty (assuming that the marine $^{234}U/^{238}U$ ratio has remained constant[32]), whereas ages with values of 149 ± 8‰ are considered to be accurate to ±2 kyr[4,6,13,14] and ages with values that exceed 149 ± 8‰ are considered to be unreliable.

Combined $^{230}Th$ and $^{231}Pa$ dating has shown that the $\delta^{234}U(T)$ criterion alone is insufficient to identify all corals affected by open-system diagenesis and that >50% of $^{230}Th$ ages with reliable isotopic values can have discordant $^{231}Pa$ ages[8]. An additional test with significant potential to screen coral ages for open-system behaviour is stratigraphic consistency. The expectation that ages in a conformable sequence should simply decrease with increasing elevation is unrealistic, as shallow reef-crest deposits are commonly mixtures of hurricane-emplaced fragments and *in situ* colonies[19]. Hurricanes therefore cause temporal mixing within individual reef-crest units as they develop, and those that have been dated at a sub-metre resolution show age reversals of up to 850 yrs[12,19]. More rigorous quantification of such extrinsic age variability in Holocene reefs[27] has recently provided a criterion to better screen isotopically reliable ages for stratigraphic consistency. This criterion is based on the finding that a minimum of three corals growing within a 3-m vertical stratigraphic interval (that is, the average amount of accretion found to occur in 1 kyr or less) should not have an age distribution of >1 kyr (limit of age resolution possible with a minimum of three coral ages). As a result, we consider the ages of groups of three or more corals that vary by no more than 1 kyr and come from conformable stratigraphic sections no thicker than 3 m to be stratigraphically reliable.

31. Gonzalez-Herrera, R., Sanchez-y-Pinto, I. & Gamboa-Vargas, J. Groundwater-flow modeling in the Yucatan karstic aquifer, Mexico. *Hydrogeol. J.* **10,** 539–552 (2002).
32. Henderson, G. M. Seawater ($^{234}U/^{238}U$) during the last 800 thousand years. *Earth Planet. Sci. Lett.* **199,** 97–110 (2002).

## 1. Supplementary Table 1. Isotopic data and $^{230}$Th ages for Xcaret coral samples

| Site | Sample (height m) | Age kyr | ± kyr | 238U ppm | ± ppm | 232Th ppb | ± ppb | 234U/238U(0) ‰ | ± ‰ | 234U/238Ui ‰ | ± ‰ | Reliability |
|---|---|---|---|---|---|---|---|---|---|---|---|---|
| 1 | 2 | 3 | | 4 | | 5 | | 6 | | 7 | | 8 |
| **xA4-xa** | *Ap clast* | **117.6** | 1.4 | **3.184** | 0.013 | **5.000** | 0.050 | 117 | 2 | 163 | 3 | u |
| **xA4-xb** | (+2.0) | **137.1** | 1.8 | **2.114** | 0.089 | **16.300** | 0.100 | 122 | 2 | 180 | 3 | u |
| **xA4-xc** | | **114.2** | 1.1 | **3.291** | 0.014 | **0.755** | 0.050 | 121 | 2 | 167 | 3 | u |
| **xA4-xd** | | **111.4** | 1.2 | **3.347** | 0.014 | **0.720** | 0.050 | 120 | 2 | 164 | 3 | u |
| **xA4-1a** | *Ap clast* | **179.0** | 2.4 | **1.155** | 0.002 | **0.198** | 0.001 | 103 | 2 | 166 | 3 | u |
| **xA4-1b** | (+1.3) | **158.9** | 1.9 | **1.169** | 0.001 | **0.318** | 0.022 | 106 | 2 | 166 | 3 | u |
| **xA4-1c** | | **567.3** | 139.1 | **1.450** | 0.002 | **0.288** | 0.021 | 96 | 2 | 527 | 3 | u |
| **xA4-2a** | *Ap colony* | **138.2** | 1.8 | **1.542** | 0.002 | **0.048** | 0.001 | 104 | 2 | 154 | 3 | u |
| **xA4-2b** | (+2.2) | **132.6** | 1.6 | **1.911** | 0.002 | **0.359** | 0.025 | 102 | 2 | 148 | 3 | sr |
| **xA4-2c** | | **134.3** | 1.4 | **1.993** | 0.003 | **0.177** | 0.020 | 101 | 2 | 149 | 3 | sr |
| **xC7-2a** | *Ss colony* | **146.0** | 1.7 | **2.637** | 0.003 | **0.135** | 0.001 | 131 | 2 | 198 | 3 | u |
| **xC7-2b** | (+1.7) | **158.2** | 1.7 | **2.624** | 0.003 | **0.168** | 0.014 | 135 | 2 | 212 | 3 | u |
| **xC7-2c** | | **149.6** | 1.4 | **2.700** | 0.003 | **0.252** | 0.019 | 135 | 2 | 206 | 3 | u |
| **xC7-2d** | | **137.4** | 2.1 | **3.250** | 0.014 | **0.568** | 0.034 | 127 | 2 | 187 | 3 | u |
| **xC7-2e** | | **137.7** | 2.2 | **3.259** | 0.013 | **1.230** | 0.043 | 127 | 2 | 187 | 3 | u |
| **xC7-5a** | *Ss colony* | **110.7** | 1.0 | **3.190** | 0.013 | **0.152** | 0.003 | 126 | 2 | 172 | 3 | u |
| **xC7-5b** | (+1.0) | **107.7** | 1.0 | **3.296** | 0.014 | **0.439** | 0.003 | 128 | 2 | 174 | 3 | u |
| **xC7-5c** | | **110.2** | 1.2 | **3.214** | 0.014 | **0.111** | 0.003 | 124 | 2 | 169 | 3 | u |
| **xD4-2a** | *Ap colony* | **117.0** | 1.0 | **2.769** | 0.003 | **0.178** | 0.001 | 105 | 2 | 147 | 3 | sr |
| **xD4-2b** | (+4.7) | **122.8** | 1.1 | **2.712** | 0.002 | **0.259** | 0.021 | 101 | 2 | 144 | 3 | r |
| **xD4-2c** | | **127.7** | 1.1 | **2.741** | 0.003 | **0.289** | 0.019 | 102 | 2 | 146 | 3 | r |
| **xD4-3a** | *Ap colony* | **119.5** | 1.1 | **2.869** | 0.004 | **1.443** | 0.003 | 100 | 2 | 148 | 3 | sr |
| **xD4-3b** | (+4.9) | **126.2** | 1.1 | **2.829** | 0.003 | **0.305** | 0.021 | 102 | 2 | 145 | 3 | r |
| **xD4-3c** | | **123.5** | 1.0 | **2.774** | 0.003 | **0.279** | 0.020 | 102 | 2 | 145 | 3 | r |
| **xE2-2a** | *Ap colony* | **117.7** | 1.1 | **3.500** | 0.015 | **0.571** | 0.004 | 112 | 2 | 156 | 3 | r |
| **xE2-2b** | (+4.0) | **121.9** | 1.2 | **2.960** | 0.012 | **0.075** | 0.002 | 115 | 2 | 162 | 3 | u |
| **xE2-2c** | | **118.4** | 1.0 | **3.280** | 0.014 | **0.328** | 0.004 | 123 | 2 | 172 | 3 | u |
| **xE3-1a** | Ap clast | **123.8** | 1.4 | **2.982** | 0.004 | **0.080** | 0.001 | 104 | 2 | 148 | 3 | sr |
| **xE3-1b** | (+3.9) | **123.5** | 1.0 | **2.974** | 0.003 | **0.102** | 0.019 | 103 | 2 | 147 | 3 | sr |
| **xE3-1c** | | **126.4** | 1.1 | **2.933** | 0.003 | **0.118** | 0.020 | 102 | 2 | 145 | 3 | r |
| **xE4-1a** | *Ap clast* | **112.3** | 0.8 | **2.807** | 0.003 | **0.209** | 0.001 | 99 | 2 | 136 | 3 | u |
| **xE4-1b** | (+4.2) | **125.4** | 1.2 | **2.621** | 0.003 | **0.148** | 0.022 | 103 | 2 | 147 | 3 | sr |
| **xE4-1c** | | **120.8** | 1.1 | **2.819** | 0.004 | **0.075** | 0.021 | 102 | 2 | 143 | 3 | r |

NOTE: Statistical errors are two standard deviations of the mean (2σ). *Column 1:* replicate analyses on sub-samples are indicated by a, b and c etc. *Column 2:* Coral samples are *Acropora palmata* (Ap) or *Siderastrea siderea* (Ss) and are either clasts or in-place colonies as noted. All coral samples are >99% aragonite based on XRD measurements (detection limit <1%). *Column 3*: ages are calculated using the equation: $(^{230}Th/^{238}U)_{act.}=1-\exp(-\lambda_{230Th}xT)+(\delta_{234}U(0))x0.001(\lambda_{230Th}/(\lambda_{230Th}-\lambda_{234U}))x(1-\exp((\lambda_{234U}-\lambda_{230Th})xT))$. Decay constants: $\lambda_{234U}$: $2.8263x10^{-6}$ yr$^{-1}$; $\lambda_{238U}$:$1.5513x10^{-10}$ yr$^{-1}$; $\lambda_{230Th}$: $9.158x10^{-6}$ yr$^{-1}$ (see ref 30). Samples are corrected for blanks and inherited $^{230}$Th associated with detrital $^{230}$Th assuming that the $^{230}Th/^{232}Th$ activity ratio is 0.6 ± 0.2. *Column 6*: measured ($^{234}U/^{238}U$) activity ratios ($\delta^{234}U(0)$) and ($\delta^{234}U(T)$) are presented as deviation per mil (‰) from the equilibrium value. *Column 7*: decay corrected ($^{234}U/^{238}U$) activity ratios ($\delta^{234}U(T)$) are calculated from the given ages and with $\lambda_{234U}$: $2.8263x10^{-6}$ yr$^{-1}$. *Column 8*: Ages are strictly reliable (sr) having pristine $\delta^{234}U(T)$ values between 146.6 ‰ and 149.6 ‰; reliable (r) with values of 149.6 ± 8‰ reflecting ages within 2 kyr of the true age; unreliable (u) with values >149 ± 8‰[6,13].

## 2. Profiles through LIG reef crests at Xcaret.

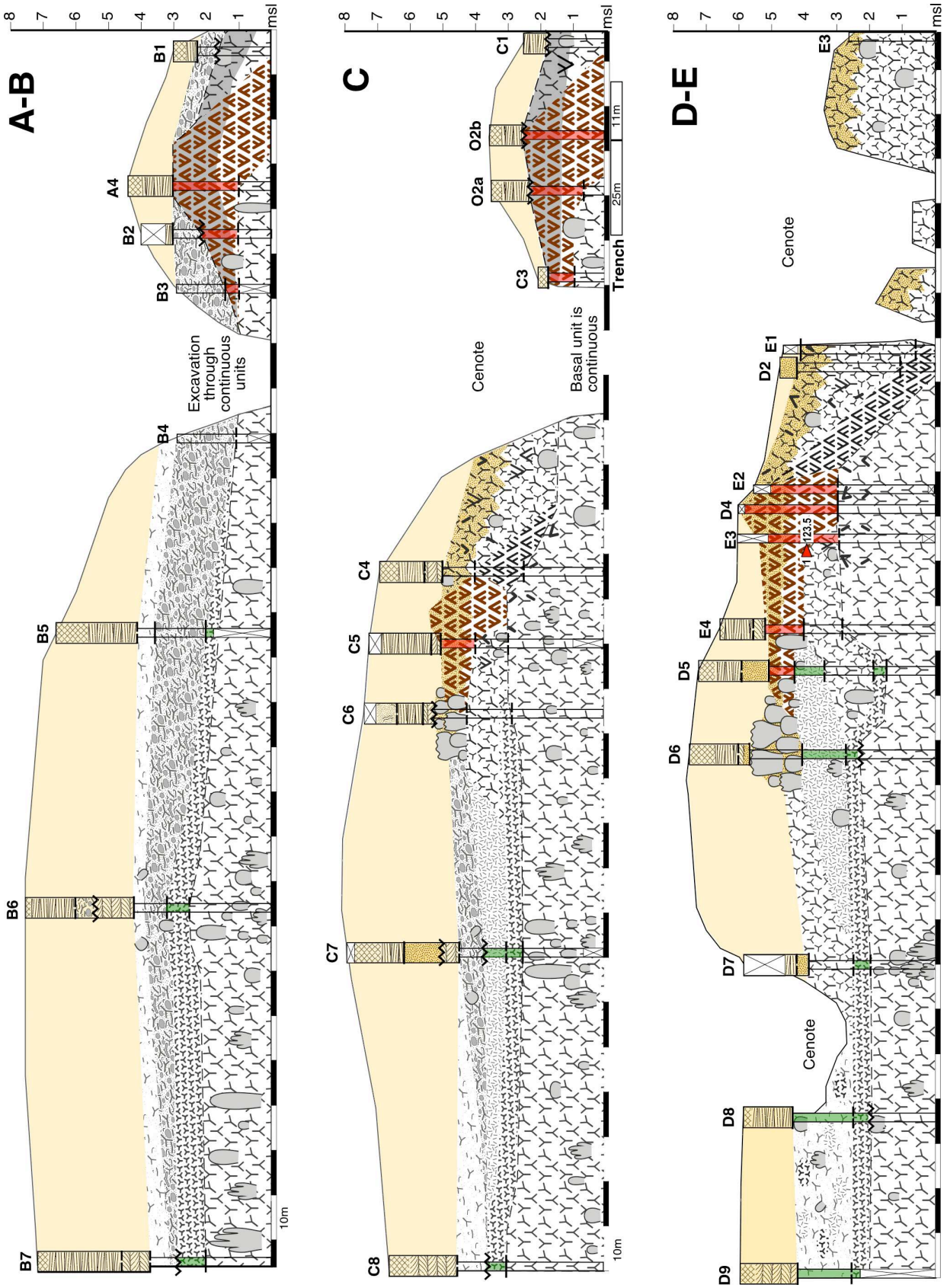

**Supplementary Figure 1. Profiles through the LIG reef tracts at Xcaret.** Stratigraphic sections along three shore-normal transects at Xcaret superimposed on scaled reconstruction of reef development (section locations and symbols shown in Fig. 1). Highlighted in red are reef-crest and reef flat units and those units in green are composed of a sediment tolerant assemblage. In the north-east, transect A-B shows the lower-reef crest passing into the lagoonal patch-reef complex. This complex disappears further north and is replaced by a lagoonal sand section. A distinctive coral-gravel storm deposit flanks the reef-crest and caps the lagoonal section, but abruptly disappears to the north. To the south it also caps the upper lagoonal unit (as seen in transect C) but pinches out shortly thereafter. Given its presence in the upper reef-tract lagoon, this storm unit clearly post-dates lower reef-tract development and demise and thereby confirms the younger age of the upper reef-tract and supports a back-stepping reef architecture. Transect C is located at the closest point between lower- and upper-reef tracts and reef-crest units in each tract disappear to the south and north respectively. For this reason both reef crests show slightly lower elevations; more representative elevations occur in the other transects. But this transect clearly shows the differences between reef-crest units: the lower unit has pore space occluded by crustose corallines whereas the upper unit is infiltrated by overlying beach deposits. This indicates that the coral assemblage in the lower crest unit had died and was encrusted by the time the upper unit developed, and that the upper crest unit had an open framework and was alive shortly before sea level fell from the highstand. Transect D-E shows the transition from the lower patch-reef complex into the upper-reef tract. Beneath the upper-reef crest, the transition is characterised by continuous coral growth and reef accretion but further into the lagoon the transition is discontinuous and erosional. This discontinuous erosion must therefore be of marine origin and cannot be the result of sub-aerial exposure following sea-level fall. Note that apart from transect A, which was subjected to excavation, the other transects are broken by a discontinuous series of cenotes that developed along a shore-parallel fracture system that likely resulted from hydrostatic unloading during the glacial lowstand; locally continuous sections across this fracture show no vertical displacement and confirm the lateral continuity of the patch-reef complex. This continuity requires that both reef tracts are contemporaneous and formed during MIS-5e.

## 3. Supplementary Discussion

### 3a. Duration of the reef back-stepping event recorded at Xcaret

The amount of time elapsed between the demise and back-stepping of reef-crest units at Xcaret can be constrained using both age and paleoecological data. The age of the +3 m reef-crest demise at Xcaret within the LIG is not well constrained from the our samples, likely due to the proximity of the reef to the water table, but elsewhere this +3 m stage of reef-crest development has been well dated[4-6]. As shown in Fig. 3, reliable and stratigraphically-consistent ages from +3 m reefs from Western Australia[5-6, 35] and reliable ages from the Bahamas[4] fall into an interval from ~126 to 121 ka. The youngest reliable age from an in-place coral in the upper-reef at Xcaret is 119.5 ka (XD4-3a). This gives a general ~ 1500 year interval in which back-stepping could have occurred. However a millennial-scale interval is inconsistent with paleoecological data which requires that back-stepping was more rapid and occurred on ecological time-scales, as outlined in the following argument:

i. The lower-crest shows no evidence of coral-community adjustment prior to its demise. This means that cessation of reef growth was ecologically rapid. Nor was the surface of the lower crest subsequently re-colonized by corals, only by a cap of coralline algae. This not only means that reef-crest corals likely suffered a mass mortality event[43], but that the environmental change was permanent. In other words, reef-crest demise and shift to another marine environment occurred rapidly on an ecological time-scale.

ii. Coral communities in distal areas of the patch-reef complex also died rapidly with no time for adjustment. They were subsequently eroded and re-colonised by a sediment-tolerant community. The erosional break, however, prevents any assessment of the timing of that community shift.

iii. But coral communities in proximal areas of the patch-reef complex were not eroded and show a continuous transition into the new environment (lower-tract lagoon to crest of upper tract) that occurred on a cm scale (see sections D4 and E2). This confirms that there was an ecologically rapid shift to a reef-crest environment ie, it occurred over the life-span of one or two generations of coral. (Note that this rapid transition was not caused by progradation of the upper-reef crest over the patch-reef complex because facies seaward and landward of the crest are composed of mixed

assemblages). In other words, reef demise and back-stepping must have occurred on an ecological time-scale.

**3b. Xcaret comparison with other LIG reef data.**

There are distinct similarities between the back-stepping reef-crests at Xcaret and fossil reefs at other LIG sites which are consistent with a late-stage sea-level jump during the highstand[33] (Supplementary Fig. 2).

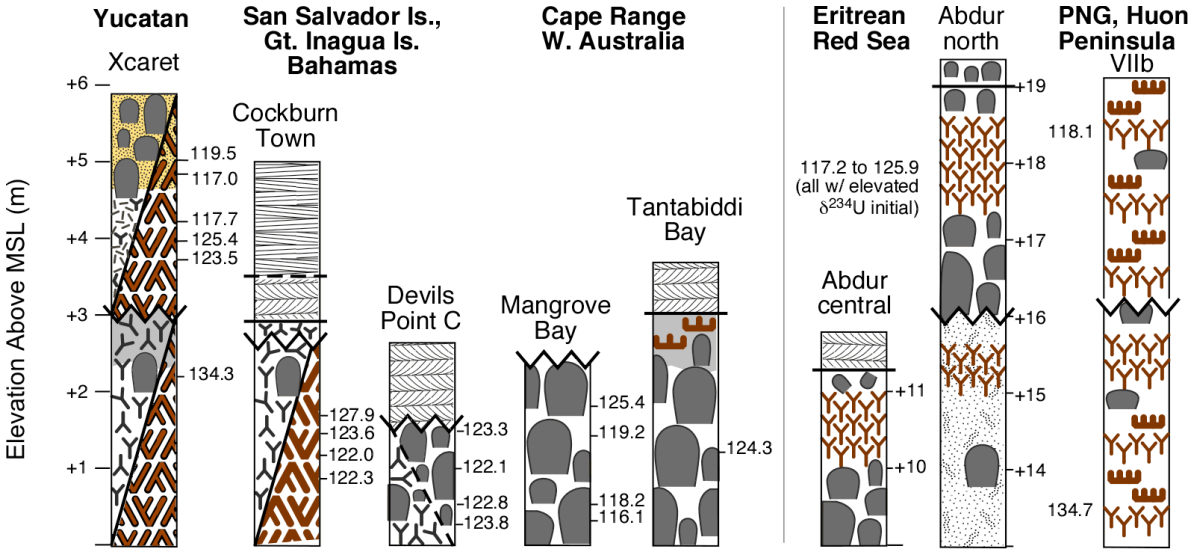


**Supplementary Figure 2.** Summary of stratigraphic sections and reliable $^{230}$Th ages from LIG reefs in stable and uplifted terranes (separated by line). Symbol key same as Fig. 1, although coral species differ in Indo-Pacific sites. (data from refs. 4,6,35,15, 14 respectively).

Along the Red Sea coast of Eritrea, an uplifted and tilted LIG reef sequence near Abdur clearly shows two superimposed stages of shallow-reef development[15]. The lower unit, composed of lagoonal sediment and patch reefs, is truncated by an intermittent marine-erosion surface and directly overlain by a reef-crest and reef-front coral assemblage. Like the sequence at Xcaret, this implies that reef-crest development back-stepped over an existing reef lagoon. Although the absolute elevation of the sequences are higher due to uplift, the elevation difference between the top of the lagoonal patch reefs and the top of the overlying reef-crest is 3 m, identical to the difference at Xcaret. But given the neotectonic setting of this site, the possibility that co-seismic uplift produced reef back-stepping cannot be discounted.

In the more stable Bahamas, several LIG sites show reef-crest *A. palmata* and lagoonal patch-reef sequences up to a maximum of +3 m[4,33,34]. Above this elevation, there is minimal reef development and sequences are dominated by lagoon and beach-sediment to > +5 m[7,34]. This reef absence, together with the preservation on several islands of pristine inter-tidal notches at +6 m, has been interpreted as evidence of a late stage, metre-scale SL excursion whose duration was too brief to permit reef development[7]. Although the Xcaret data is consistent with such an excursion, our discovery of a reef-crest sequence between +3 to +6 m indicates that there was sufficient time, therefore reef absence in

the Bahamas must be attributable to other causes.

Red Sea and Bahamian reef sequences both show the development of discontinuous marine-erosion surfaces (Supplementary Fig. 2), which have been widely accepted as evidence of emergence and sea-level fall[15,19]. In the Bahamas, for example, there is extensive evidence of marine truncation and bioerosion of corals and their clasts under these surfaces[19], but no reliable indication of emergence that can be separated from that which occurred at the end of the highstand following SL fall. This, together with poor lateral continuity and elevation below +3 m, indicates that these erosion surfaces are identical to the surface that formed following the sea-level jump at Xcaret. Continuous reef development between these surfaces at Xcaret requires an exclusively marine origin for this erosion.

In addition to the Bahamas and the Red Sea, widespread reef development up to +3 m has also been reported from stable sites along Western Australia[5,6,35] (Supplementary Fig 2). In these areas, reef development has produced a distinct and widespread terrace at +3 m. The upper surface of this reef is also reported to be capped by crustose coralline algae and some areas show the development of an extensive erosion surface below +3 m[35, 44]. Although reef framework is largely restricted to +3 m or less, the inner-margin of the terrace rises to +6 m in several stable localities[33,35,36], indicating a highstand elevation 2-3 m above the maximum reef elevation. In addition, reef development to +6 m has also been documented from restricted areas, particularly the Houtman-Abrolhos islands off the W. Australian coast[35]. Evidence also exists of a potentially higher sea-level position in Cape Cuvier [33,41], but there is uncertainty as to how this relates to the more widespread reef terrace at +3 m and unresolved questions concerning local neotectonics[6]. Nevertheless, the remarkable stratigraphic similarity between reef sequences at Xcaret and W. Australia cannot be taken as direct evidence of similar relative SL histories until reliable ages are documented from the W. Australian reefs between +3 to +6 m.

**3c. Quantifying the rate and magnitude of rapid sea-level change.**
Evidence of the rate and magnitude of sea-level change during the late Pleistocene has been documented directly using age-depth data from reef-crest and coastal sequences[9-13, 42] and indirectly using stable oxygen isotope records[17,37]. Rapid, metre-scale changes in sea level during the last deglaciation have been constrained from submerged reef-crest sequences recovered from the south coast of Barbados (Supplementary Figure 3).

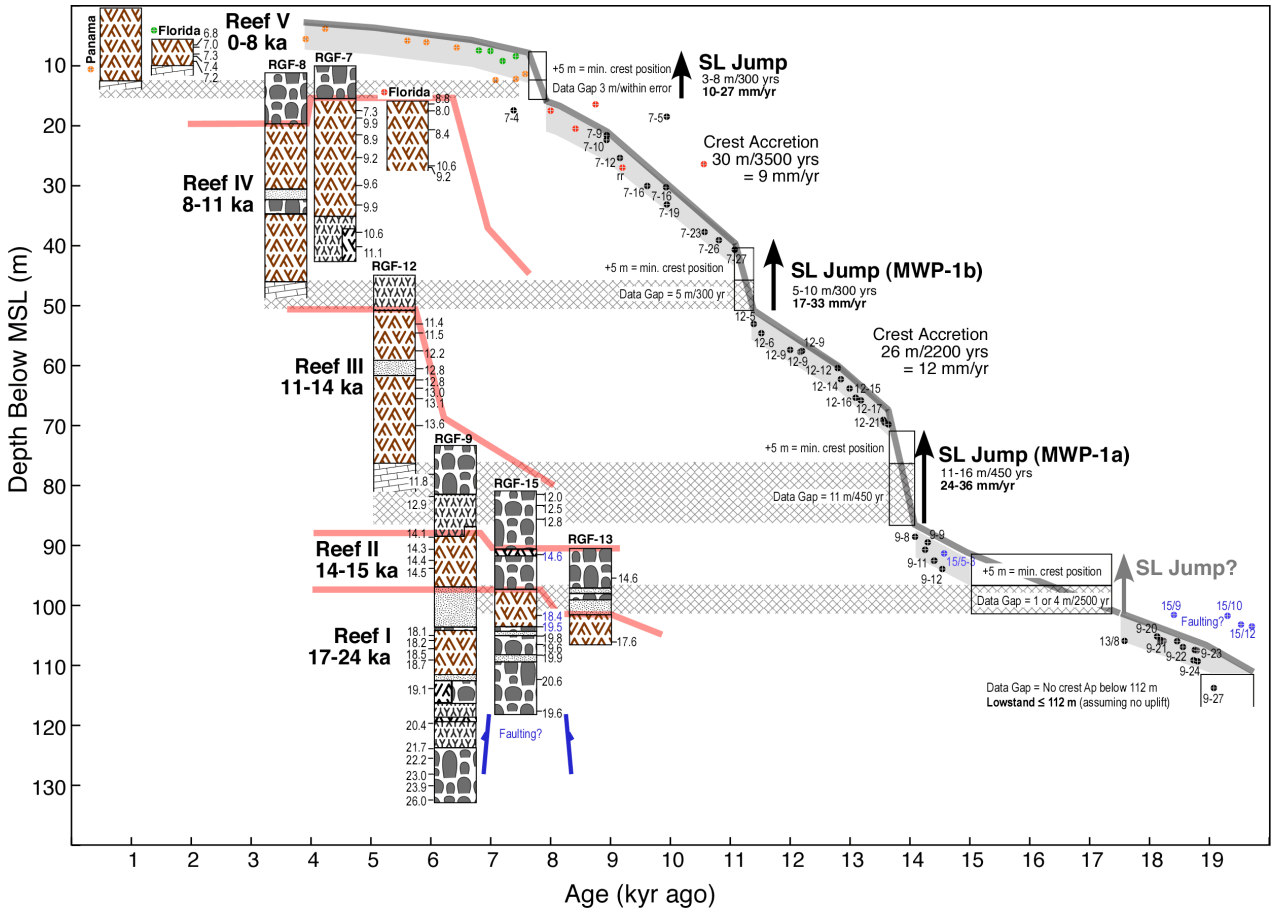


**Supplementary Figure 3. Sea-level behaviour during the last 20 kyr.** Sea level at Barbados reconstructed from elevation and thickness of back-stepping reef-crest sequences of monospecific *A. palmata*[9,10] and precise $^{230}$Th ages from corals in those sequences[28]. Also shown are the stratigraphic sequences and calibrated radiocarbon ages from relict and active Holocene reefs[12]. The position of mean sea level is reconstructed by keeping coral age/elevation data within a 5 m envelope (shaded) which represents the 0-5 m reef-crest habitat zone where *A. palmata* forms a monospecific assemblage. Outliers are either the result of localised uplift (blue data points), or up-slope transport during storms. Correction for continuous uplift of Barbados is ignored in order to quantify the rate and magnitude of sea-level jumps (arrows) that caused episodes of reef-crest drowning and back-stepping (denoted by hatching).

The Barbadian reef-crest sequences accreted vertically and maintained their sea-level position during rise rates of ~12 mm/yr. Breaks in the reef-crest sequences and resulting data gaps represent episodes when the rate of sea-level rise exceeded that accretion threshold and caused drowning of reef-crest communities and their subsequent back-stepping when rise rates subsided and allowed up-slope accretion to continue. Age-elevation data across these gaps indicate that reef drowning and back-stepping was caused by sea-level jumps (or melt-water pulses) of up to 16 m at rates of 36 mm/yr (Supplementary Fig. 3). Such rise rates provided little time for reefs to adjust to increasing water depths and, as a consequence, caused ecologically sudden drowning of reef-crest communities. Because there is an inverse relation between the rise rate and the amount of time available for accretion during submergence, such sudden drowning is manifested by limited accretion in the mixed habitat zone of *A. palmata* between 5-10 m, such that ≤ 2 m of accretion is an indication of rise-rates in excess of 45 mm/yr[10]. This concept of ecologically sudden reef-crest drowning is well illustrated in the Barbados cores by abrupt transitions from monospecific sequences of *A. palmata* to deeper-water coral assemblages and the absence of any significant thickness of mixed-zone accretion.

Rapid, metre-scale changes in sea level have also been proposed during the LIG from an isotopic reconstruction based on a sediment core (KL11) from the central region of the Red Sea[17]. This same core has also been used to reconstruct Holocene sea-level variability[37] and has been compared to the well-constrained coral-based record from Barbados, and the less well constrained record from Tahiti (Supplementary Fig. 4a). On the basis of this comparison, it was found that the KL11 δ $^{18}$O reconstruction was not able to resolve variation in sea level of less than ±12 m due to significant uncertainty in the assumptions of modelled paleo-temperature and salinity, as well as the unknown contribution of hydro-isostacy on the depth of the Hanish sill[37]. Some of these uncertainties were arbitrarily reduced for the LIG reconstruction of sea-level[17] by smoothing δ $^{18}$O data with a 750 yr running mean (Supplementary Fig. 4b). But the sea-level variation found using this method could not be validated due to the absence of similar variation in an adjacent core (KL9). Validation of the main elements of the reconstruction was therefore attempted using coral-reef data from the tectonically active shores of the Red Sea, but the number and rate and magnitude of the excursions show no similarity with well-dated coral data from stable regions (Supplementary Fig. 4b). As a result, claims concerning the rapid rate and magnitude of sea-level change during the LIG made from this isotopic reconstruction are still subject to considerable uncertainty and cannot be resolved until independent records of paleotemperature and salinity allow the sea-level component to be differentiated[37].

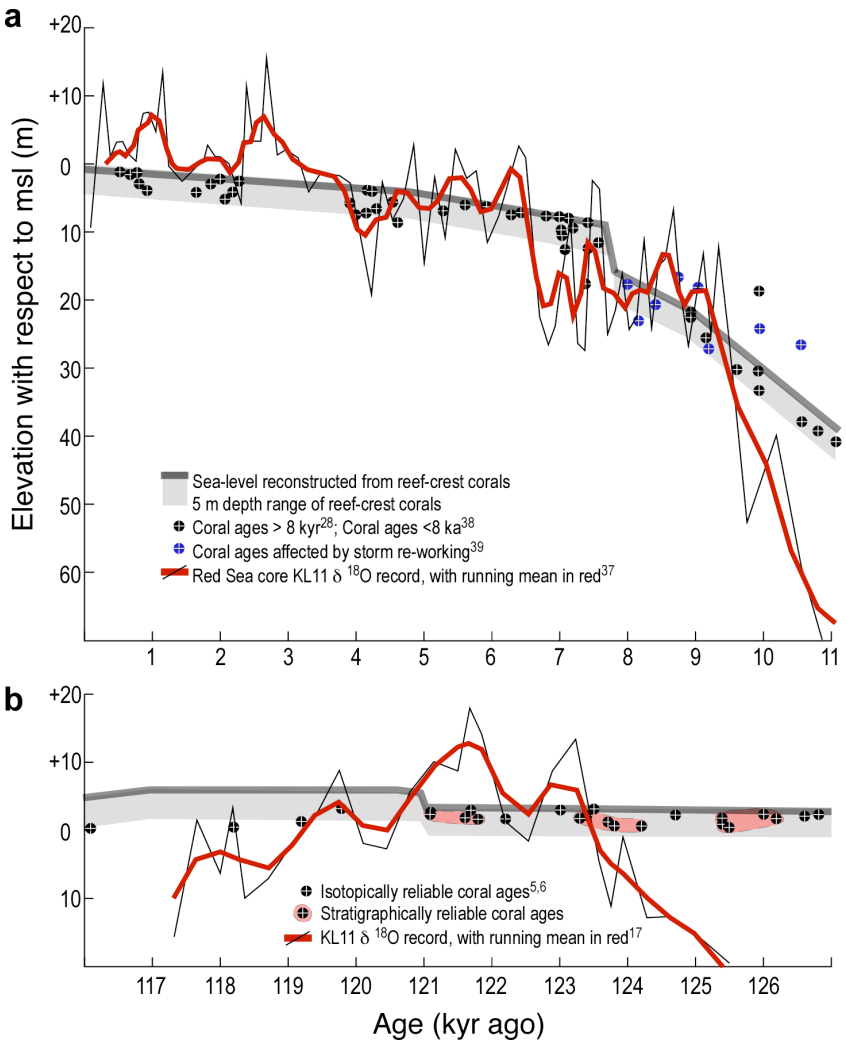

**Supplementary Figure 4. Comparison of sea-level reconstructions from coral and isotope data.** **a.** Holocene sea level from Western Atlantic reef-crest corals[38,39] showing a gradual rise punctuated by a jump at ~8 kyrs[12,40]. Overlying this record is the stable oxygen-isotope reconstruction of sea level over the same interval from the Red Sea[37]. Note that the Red Sea record shows significantly higher variation due to uncertainty in modelling the influence of paleotemperature and salinity[37]. This variation produces sea-level excursions of 10-15 m which are not reflected in the coral record. **b.** Comparison of coral-based sea level from W. Australia[5,6] during the LIG and an isotopic reconstruction over the same interval from the same Red Sea core[17]. Again the isotopic reconstruction shows significantly higher variation producing sea-level excursions of 10-15 m which are not reflected in the coral record.

33. Hearty, P., Hollin, J., Neumann, A., O'Leary, M. & McCulloch, M. Global sea-level fluctuations during the Last Interglaciation (MIS 5e). *Quat. Sci. Rev.* **26**, 2090-2112 (2007).

34. Hattin, D.E. & Warren, V.L. Stratigraphic analysis of a fossil Neogoniolithon-capped patch reef and associated facies, San Salvador, Bahamas. *Coral Reefs* **8**, 19-30 (1989).

35. Eisenhauer, A. *et al*. The Last Interglacial sea level change: new evidence from the Abrolhos islands, West Australia. *Geol Rundsch.* **85,** 606-614 (1996).

36. Murray-Wallace, C.V. & Belperio, A.P. The Last Interglacial shoreline in Australia: A review. *Quat. Sci. Rev.* **10**, 441-46l (1991).

37. Siddall, M. *et al.* Understanding the Red Sea response to sea level. *Earth Planet. Sci. Lett.* **225**, 421– 434 (2004).

38. Toscano, M.A., Macintyre, I.G. Corrected western Atlantic sealevel curve for the last 11,000 years based on calibrated $^{14}C$ dates from *Acropora palmata* framework and intertidal mangrove peat. *Coral reefs* **22**, 257–270 (2003).

39. Lighty, R.G., Macintyre, I.G. & Stuckenrath, R. Submerged early Holocene barrier reef south-east Florida shelf. *Nature* 275, 59-60 (1978).

40. Yu, S.Y., Berglund, B.E., Sandgren, P. & Lambeck, K. Evidence for a rapid sea-level rise 7600 yr ago. *Geology* **35**, 891-894 (2007).

41. O'Leary, M., Hearty, P. & McCulloch, M. Geomorphic evidence of major sea-level fluctuations during marine isotope substage-5e, Cape Cuvier, Western Australia. *Geomorphology*, doi:10.1016/j.geomorph.2008.06.004 (2008).

42. Yokoyama, Y., Lambeck, K., De Deckker, P., Johnston, P., Fifield, L.K. Timing of the Last Glacial Maximum from observed sea-level minima. Nature 406, 713-716.

43. Pandolfi, J.M. et al. Mass mortality following disturbance in Holocene coral reefs from Papua New Guinea. Geology 34, 949-952 (2006).

44. Greenstein, B.J., Pandolfi, J.M. & Blakeway, D.R. A fossil reef from the last interglacial, Western Australia. Coral Reefs 24, 593 (2005).